Different Modes of a Capacitively Coupled Radio-Frequency Discharge in Methane

I. V. Schweigert*

Institute of Theoretical and Applied Mechanics, 630090 Novosibirsk, Russia

(Received 17 May 2003; published 15 April 2004)

The transition between different regimes of a capacitevely coupled radio-frequency gas discharge in methane is studied with a combined particle-in-cell Monte Carlo collision algorithm over a wide range of gas pressure P and discharge current j. The results of this study are compared with known experimental and numerical results and summarized on a P-j phase diagram, which constitutes the areas of existence of different discharge regimes.

DOI: 10.1103/PhysRevLett.92.155001 PACS numbers: 52.27.Aj, 52.65.Ww, 52.80.Pi

The existence of different regimes of the capacitevely coupled radio-frequency (ccrf) discharge glow was first reported by Levitskii [1]. Since this pioneering work, the transition between the low power and high power discharge modes is attributed to so-called α-γ transition. The features of these discharge modes are the following: at the low ccrf discharge voltage (α mode) the ionization is provided by the bulk plasma electrons, whereas at the high discharge voltage the ionization is maintained by the secondary electrons from the electrodes due to the ion bombardment (γ mode). A sharp rise of the electron density and the drop of the electron temperature are supposed to be induced by the secondary electrons. Godyak *et al.* [2] have studied experimentally the transition between the low voltage and high voltage modes in argon and helium. In kinetic simulations [3] and in calculations with a two-electron group fluid model [4], the α-γ transition in a rf discharge was studied in helium. Another type of electron heating-mode transition was found in the experiment in a low pressure argon discharge [5] and associated with the Ramsauer effect. In the ccrf discharge in silane the transition was studied experimentally [6,7] and numerically [8]. It was found that in the volume dominated mode the α-Si:H deposition rate drastically increased. Recently, in spite of many practical applications of the ccrf discharge in technological processes, for instance for the diamond like carbon film deposition, a basic understanding of transition in *molecular* gases, is still incomplete.

In this Letter we study the transition between two modes of the ccrf discharge in methane, using the algorithm [9] that combines the fluid model and the particle-in-cell Monte Carlo collision (PIC-MCC) technique. The drawback of the pure fluid model is that the inertia of charged species is neglected, which restricts the validity of this approach by the higher gas pressure range. On the other hand, in the PIC-MCC simulation the large number of the simulation particles are needed, and at low P the statistical fluctuations of electric field lead to the artificial heating of electrons. In our combined PIC-MCC model [9], the electron and ion kinetic equations [three dimensional over velocity and one dimensional (1D) in space], the transport equation for electron and ion densities and fluxes, and the Poisson equation are solved self-consistently. The kinetic approach allows us to find the kinetic coefficients, and the electric field distribution is found from the auxiliary equations. The advantage of our new approach is a visible acceleration of the PIC-MCC simulations, which is reached due to a considerable decrease of the number of simulation particles N. We use only $N = 5000$ for all P without increasing of statistical noise, whereas the standard PIC-MCC algorithm [10] needs more than $N = 256\,000$ simulation particles at the low gas pressure to obtain the reasonable accuracy (see Ref. [9]).

We consider a 1D symmetrical ccrf discharge with 13.56 MHz frequency. One electrode is grounded, and the voltage on another electrode is calculated self-consistently to provide the desired current j. We choose the current as an input parameter following the experimental conditions of Refs. [2,5]. Interelectrode distance $d = 3$–6 cm and the spatial grid has 81–131 nodes, condensing in electrode sheaths. For simplicity, following Ref. [11], we consider only an ion CH_5^+. The methane is treated like electropositive gas [12]. The model of electron kinetics in methane includes electron-neutral collisions [11,12] and electron Coulomb collisions [13]. The ion-neutral collisions are supposed to be charge exchange processes. Here we will not discuss the plasma chemistry, which is out of this article scope.

Varying the discharge parameters, we observe two different regimes of a ccrf discharge glow. The typical distributions of the electron density n_e and the electron energy ϵ averaged over discharge cycles are shown in Fig. 1. The first, the volume dominated (VD) regime, is characterized with the low plasma density, the high electron energy (curves 1 and 4 in Fig. 1), and the higher power input. The electron energy distribution has the usual shape of a plateau. The second, the active sheath (AS) regime of the discharge glow (curves 2, 3, and 5 in Fig. 1), has much higher n_e. The electron energy profile exhibits two maxima in the sheaths adjacent to the electrodes and a deep minimum in the center of the discharge. In Fig. 1 we also show n_e and ϵ measured in Ref. [14]. In

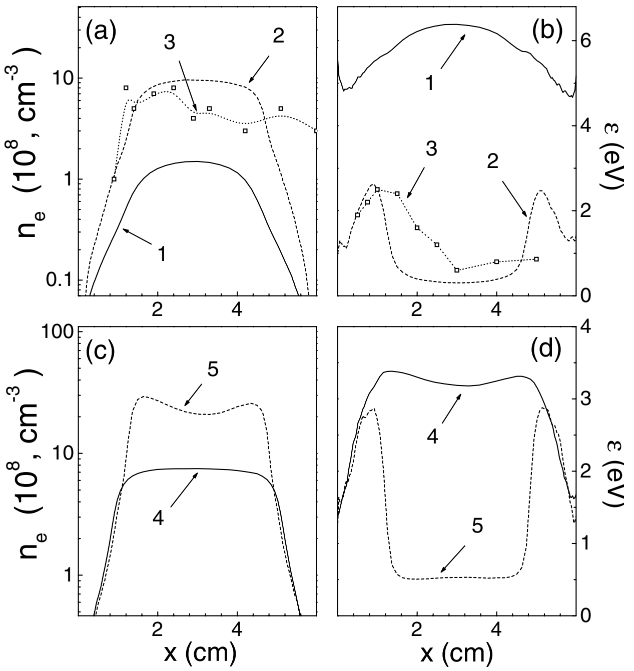

FIG. 1. Averaged over time distributions of electron density n_e (a),(c) and electron energy ϵ (b),(d) over discharge gap. Computed n_e and ϵ for $j = 0.45$ mA/cm^2 and $P = 0.01$ Torr (curve 1) and for $j = 0.45$ mA/cm^2 and $P = 0.123$ Torr (curve 2). Measured n_e and ϵ from Ref. [14] (curve 3) for discharge power 5 W and $P = 0.123$ Torr. Computed n_e and ϵ for $P = 0.075$ Torr and $j = 1$ mA/cm^2 (curve 4) and for $P = 0.075$ Torr and $j = 1.1$ mA/cm^2 (curve 5).

simulation the altering of j and P changes the discharge characteristics monotonically up to some critical point. The transition takes place abruptly and is accompanied with considerable modification of ϵ and n_e profiles, as well as the discharge power. As seen in Figs. 1(c) and 1(d) a slight change of j from 1 to 1.1 mA/cm^2 switches the system from the VD regime to the AS one.

In previous studies this change of regimes was associated with the α-γ transition, and we analyzed the influence of the secondary electrons on the discharge dynamics. We assumed that the coefficient of the electron-ion emission $\gamma = 0$–0.5 and the initial energy of the secondary electrons $\epsilon = 1$ eV. The results of our simulation with various γ have shown that even for the extra large $\gamma = 0.5$ the transition current j^* becomes only 25% less than j^* with $\gamma = 0$. The discharge always glows in the α regime at $P = (0.01$–$1)$ Torr and $j = (0.45$–$2.2)$ mA/cm^2. For the ccrf discharge operating in methane, consequently, the α-γ mechanism is not *responsible* for the transition between different modes. In molecular gas the electron energy relaxation length λ is much smaller than λ in noble gases due to excitation of vibration states with low threshold energies (0.162 eV, 0.36 eV). The secondary electrons from the electrodes, therefore, are not able to form a high energy beam like in a noble gas discharge in the γ regime. Figure 2 shows the electrons energy probability function (EEPF) before and after transition. Belonging to the AS regime, the EEPF in the sheath has the tail of electrons with energy higher than the ionization thresholds (12.6 and 14.3 eV). These hot electrons are able to provide the sufficient ionization rate within the electrode sheaths to support the chosen current. The electrons in the center of the discharge gap play a passive role. Unlike the AS regime, in the VD regime the lack of the ionization rate in the sheath is compensated by the ionization in the bulk plasma. The EEPF in Fig. 2 (see inset) demonstrates a small amount of electrons with ionization capability in the VD regime both in the center and in the sheaths. Figure 3 shows the electron heating and cooling for these two regimes. The difference in the electron kinetics is that in the VD mode the electrons gain additional energy in the central part of the discharge, whereas in the AS regime the electrical field in the bulk plasma is very small, and ϵ drops here up to a fraction of an electron volt. Here the thermalized electrons are trapped by the potential well and plasma density increases as predicted in Ref. [15]. As seen in Figs. 3(c) and 3(d), the dissociation processes are more pronounced in the VD regime. A similar phenomenon was observed in Ref. [6] in the silane discharge. In the particular case of $d = 6$ cm, the largest part of electron energy dissipates through the excitation of vibration states of CH_4 molecules. The reduction of the gap results in a more efficient redistribution of the discharge power and an increase of dissociation rate.

To identify the location of the VD and AS regimes, we calculated the ccrf discharge dynamics over a wide range of plasma parameters. The results of this study for the growing current branch are summarized in the phase

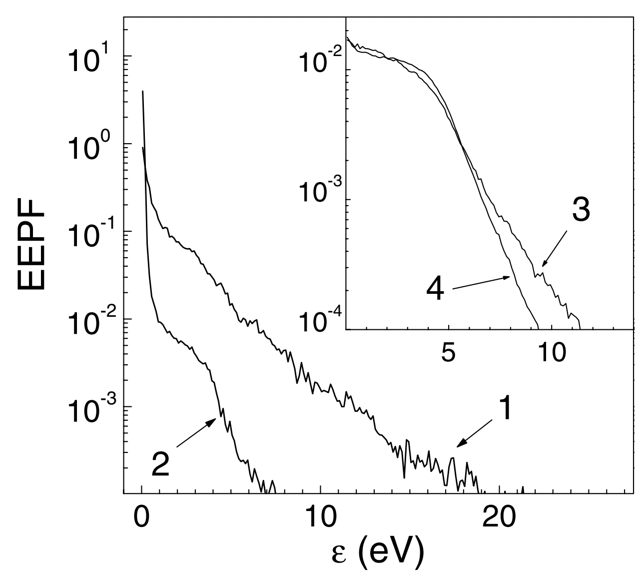

FIG. 2. Electron energy probability function for $j = 1.1$ mA/cm^2 at $x = 0.86$ cm (curve 1) and at $x = 3$ cm (curve 2) and for $j = 1$ mA/cm^2 at $x = 1.36$ cm (curve 3) and at $x = 3$ cm (4) (inset) for $P = 0.075$ Torr and $d = 6$ cm.

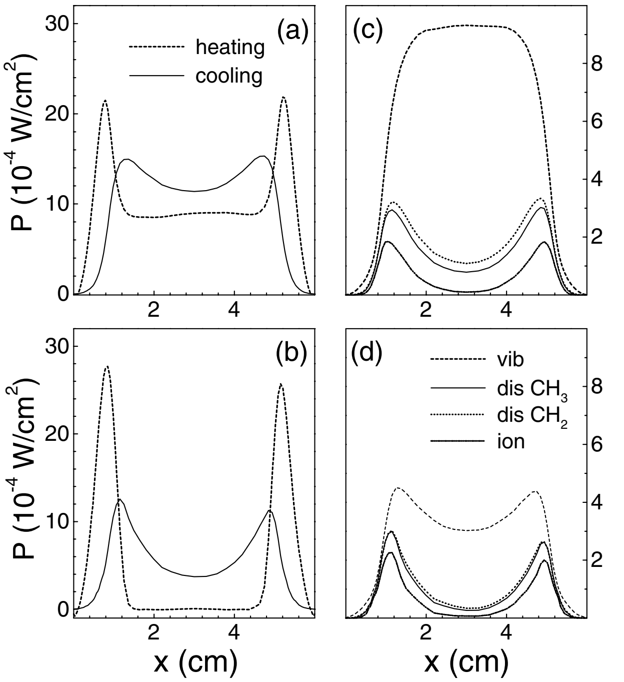

FIG. 3. Distribution of averaged over time total electron heating (dashed lines) and cooling (solid lines) (a),(c) and electron cooling due to excitation of vibration states (dashed lines), dissociation for CH_3 (solid lines) and for CH_2 (dotted lines) and ionization (dot-dashed lines) (b),(d) for $j = 1\ \mathrm{mA/cm^2}$ (a),(c) and for $j = 1.1\ \mathrm{mA/cm^2}$ (b),(d) at $P = 0.075$ Torr.

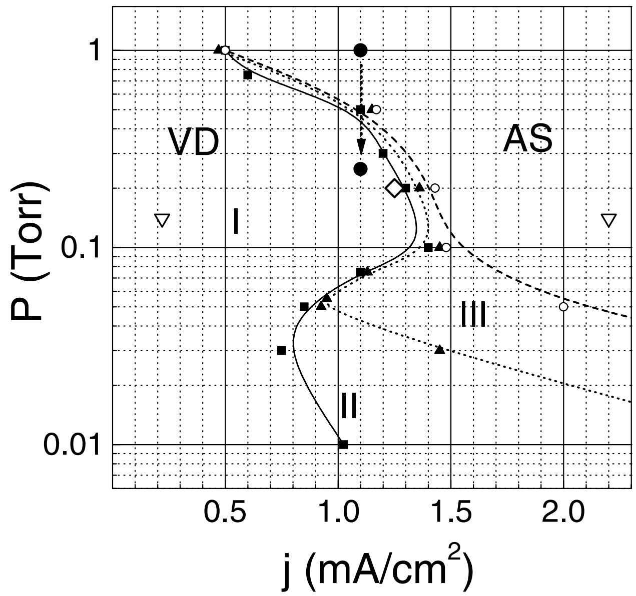

FIG. 4. Phase diagram of different regimes of ccrf discharge in methane for $d = 6$ cm (solid line), 4 cm (dotted line), and 3 cm (dashed line); results from Ref. [16] (open triangles), Ref. [11] (diamond), and Ref. [18] (solid circles).

diagram of Fig. 4. In it we show the location of the VD mode and the AS mode as a function of j and P for different d. In simulation we started from the low j and first observed the VD regime. While *increasing* the current, we reached a critical point and the discharge switched to the AS mode. In Fig. 4 area I refers to the location of the VD regime for $d = 6$ cm. For smaller d, the VD regime spreads out over the phase diagram. For $d = 4$ cm the VD regime already consists of areas I and II. The further reduction of the gap up to 3 cm adds area III, and now at $P < 0.05$ Torr the discharge always glows in the VD mode. The results of previous studies of the methane ccrf discharge are also shown in Fig. 4. In Ref. [16] the VD and AS regimes were found in simulations with $j = 0.2$ and $2.2\ \mathrm{mA/cm^2}$ ($P = 0.14$ Torr and $d = 3$ cm) (open triangles in Fig. 4). The computed discharge structure from Ref. [17] for $P = (0.1\text{–}0.35)$ Torr, $j = 3\ \mathrm{mA/cm^2}$, and $d = (3.5\text{–}6.5)$ cm corresponds to the AS mode. The VD regime was found in Ref. [11] for the discharge voltage $U = 275$ V, $P = 0.2$ Torr, and $d = 3.5$ cm (diamonds in Fig. 4). In Ref. [18] the discharge is treated on the basis of the 2D fluid model. At $U = 100$ V a decrease of P from 1 to 0.25 Torr initiates the transition from the corner dominate regime to the volume dominated one. At this transition n_e decreases and ϵ essentially increases over all discharge volume. In our 1D combined PIC-MCC simulations, we take the same gap $d = 4$ cm and $U = 100$ V. Changing P from 1 to 0.25 Torr, we also observed a drop of n_e and a rise of ϵ, which refers the transition between the AS and VD modes. The transition found in Ref. [18] fits our phase diagram perfectly (solid circles in Fig. 4).

The results presented above were obtained for the growing current branch when the chosen current is approached from "below." The attempt to reach the chosen current from "above" by decreasing j gave us unexpected results. We have obtained another steady-state solution. In Fig. 5 n_e and ϵ in the center of discharge are shown for the

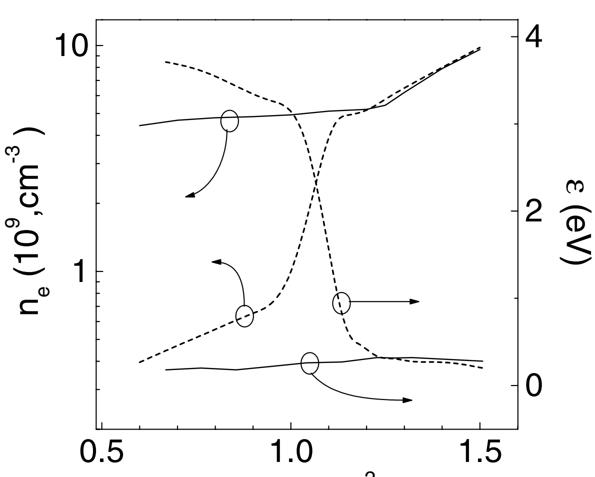

FIG. 5. Time averaged electron energy and electron density as function of j for $P = 0.075$ Torr and $d = 6$ cm. Growing current branch (dashed lines) and falling current branch (solid lines).

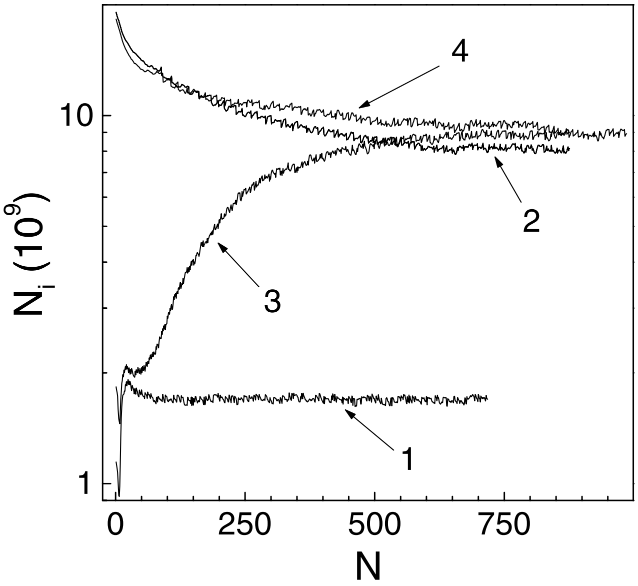

FIG. 6. Total ionization as a function of the number of discharge periods for $j = 0.7$ mA/cm^2 from below (curve 1) and from above (curve 2), and for $j = 0.75$ mA/cm^2 from below (curve 3) and from above (curve 4), for $P = 0.03$ Torr and $d = 6$ cm.

growing and *falling* current branches. Along the growing branch, at lower currents, we observe the VD regime up to the critical current 1.1 mA/cm^2. After transition to the AS regime ϵ drops and n_e significantly rises. Along the falling current branch at high current the discharge glows in the AS mode and with decreasing j, the AS mode survives up to very low current values. In the experiment such a hysteresis was observed in Ref. [6] in the silane discharge. To understand the mechanism of transition between the VD and AS modes, we calculated the total number of ionization events N_i, which is shown in Fig. 6 for $j = 0.7$ and 0.75 mA/cm^2 at $P = 0.03$ Torr ($j^* = 0.725$ mA/cm^2). It is seen that after transition at $j = 0.75$ mA/cm^2, N_i increases by 1 order of magnitude. However, the variation of j from 0.75 to 0.7 mA/cm^2 does not change much the total ionization N_i. It is clear that the transition is initiated by a quick rise of ionization in the sheath [19]. In order to maintain the AS mode, in contrast to the VD mode, a much higher ionization rate is needed. The occurrence of hysteresis is explained by the existence of two steady-state solutions (two different modes) within some range of j. The choice of the discharge to glow in one of these two modes depends on the prehistory of the system. When the transition from the VD mode to the AS mode takes place (growing current branch), in the VD mode the electron density $n_e^{\rm VD}$ is comparably low. The sheath electrical field, therefore, should be sufficiently large to provide the energy higher than the ionization threshold for the main part of electrons. If j changes along the falling current branch, in the AS mode the electron density $n_e^{\rm AS} \gg n_e^{\rm VD}$. In this case the high level of ionization, which is necessary for the AS mode, could be maintained at a lower sheath electric field. Thus, the transition from the AS regime to the VD one occurs at a lower value of j^* than the transition between the VD and AS regimes. This behavior (hysteresis) is not due to properties of gas methane. It is general property for high-frequency discharges operating in two different modes.

In conclusion, we have systematically studied two regimes of the ccrf discharge glow in methane and constructed the P-j phase diagram to show the location of the VD and AS regimes. The critical values for transition have first been calculated for a wide range of j and P. The transition between two modes of the discharge have been shown to be not related to the α-γ transition like in the argon discharge. We have found the hysteresis in the discharge behavior. By increasing the current or decreasing one up to a chosen current value, we have obtained different regimes of the discharge glow.

I wish to thank A. Smirnov and A. Alexandrov for fruitful discussions. This work is supported by the NATO Science for Peace Program, Grant No. 974354.

*Electronic address: ischweig@itam.nsc.ru

[1] S. M. Levitskii, Zh. Tekh. Fiz. **27**, 1001 (1957) [Sov. Phys. Tech. Phys. **2**, 887 (1957)].
[2] V. A. Godyak, R. B. Piejak, and B. M. Alexandrovich, Phys. Rev. Lett. **68**, 40 (1992).
[3] G. J. Parker *et al.*, Phys. Fluids B **5**, 646 (1993).
[4] Ph. Belenguer and J. P. Boeuf, Phys. Rev. A **41**, 4447 (1990).
[5] V. A. Godyak and R. B. Piejak, Phys. Rev. Lett. **65**, 996 (1990).
[6] C. Bohm and J. Perrin, J. Phys. D **24**, 865 (1991).
[7] J. L. Andujar *et al.*, J. Vac. Sci. Technol. A **9**, 2216 (1991).
[8] J. P. Boeuf and Ph. Belenguer, J. Appl. Phys. **71**, 4751 (1992).
[9] I. V. Schweigert and V. A. Schweigert, arxiv.org/abs/physics/0308071 [Plasma Sources Sci. Technol (to be published)].
[10] C. K. Birdsall and A. B. Langdon, *Plasma Physics Via Computer Simulation*, (McGraw-Hill, New York, 1985).
[11] K. Nagayama, B. Farouk, and Y. H. Lee, IEEE Trans. Plasma Sci. **26**, 125 (1998).
[12] E. Gogolides *et al.*, Jpn. J. Appl. Phys. **34**, 261 (1995).
[13] W. M. Manheim, M. Lampe, and G. Joyce, J. Comput. Phys. **138**, 563 (1997).
[14] H. Sugai *et al.*, Appl. Phys. Lett. **56**, 2616 (1990).
[15] S. V. Berezhnoi, I. D. Kaganovich, and L. D. Tsendin, Plasma Phys. Rep. **24**, 556 (1998).
[16] V. Ivanov *et al.*, J. Appl. Phys. **91**, 6296 (2002).
[17] K. Bera, B. Farouk, and Y. H. Lee, Plasma Sources Sci. Technol. **10**, 211 (2001).
[18] K. Bera, B. Farouk, and Y. H. Lee, Plasma Sources Sci. Technol. **8**, 412 (1999).
[19] To check this statement in calculations, the threshold of ionization cross section σ_i^* was shifted over the energy. As a result, the critical j^* increased if σ_i^* was shifted to the larger energy (+ 0.5 eV) and decreased if σ_i^* refers to lower energy (− 0.5 eV).